

the availability of an ambient pressure (up to 10 mbar) soft X-ray spectroscopy endstation at **TLS 24A1** added a new impetus to the research. Chun Chung Chan from National Taiwan University and his co-workers investigated the phase transformation from ACC to calcite in the presence of ambient water vapor using the Ca L-edge XAS technique *in situ*.¹

As shown in **Fig. 1(a)**, when the hydrated ACC sample was heated under ultrahigh vacuum (UHV) toward 773 K to remove water of hydration, Ca L edge XAS spectra underwent small changes. In contrast, Ca L edge spectra for the hydrated ACC heat-treated to 773 K in the presence of 0.4 mbar exhibited richer spectral changes, as shown in **Fig. 1(b)**. Careful fitting of the XAS put the CFS parameter changes on a firmer footing, as summarized in **Fig.**

2. These data indicate that crystallization is promoted in the presence of water vapor; ACC of type 2 cannot be simply equated to anhydrous ACC and is in fact more structurally similar to commercial nano-calcite. A revised path of formation is depicted as follows: hydrated ACC → disordered nano-calcite → biogenic calcite. (Reported by Chia-Hsin Wang and Yao-Wen Yang)

*This report features the work of Chun Chung Chan and his co-workers published in Chem. Commun. **55**, 6946 (2019).*

TLS 24A1 BM – (WR-SGM) XPS, UPS

- UHV-XPS, AP-XPS, UPS, XAS-based on Electron Detection Modes
- Surface Science, Chemical State of the Material Surface, Catalytic Reaction

References

1. C. Tsao, P.-T. Yu, C.-H. Lo, C.-K. Chang, C.-H. Wang, Y.-W. Yang, J. C.-C. Chan, *Chem. Commun.* **55**, 6946 (2019).
2. Y. U. T. Gong, C. E. Killian, I. C. Olson, N. P. Appathurai, A. L. Amasino, M. C. Martin, L. J. Holt, F. H. Wilt, P. U. P. A. Gilbert, *Proc. Natl. Acad. Sci.* **109**, 6088 (2012).

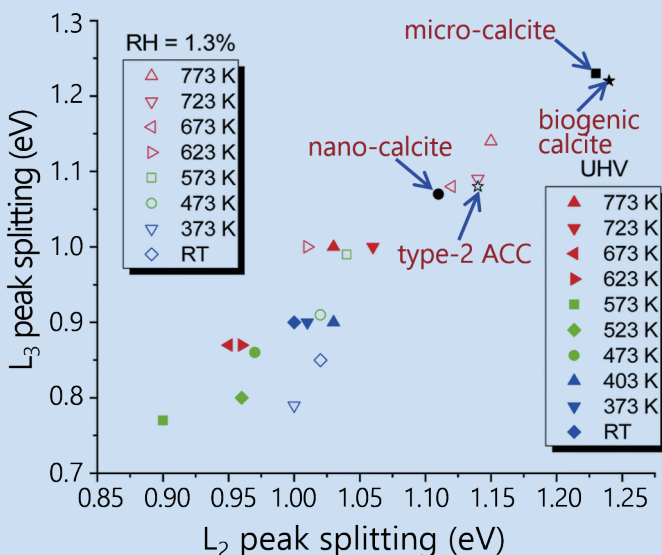


Fig. 2: CFS splittings of Ca L₂ and L₃ absorptions extracted from the spectra shown in **Fig. 1**. The filled symbols represent the data acquired under UHV (**Fig. 1(a)**); the open ones denote the data at RH 1.3% (**Fig. 1(b)**). The blue, green and red colors represent the temperature range in which the samples corresponded to hydrated ACC, anhydrous ACC and calcite in the TGA-DSC measurements. Also marked on the figure are the data corresponding to four other samples: type-2 ACC, biogenic calcite,² commercial nano-calcite, synthetic micro-calcite. [Reproduced from Ref. 1]

Membranes Comprising Metal-Organic Frameworks for Gas Separation

Organic photovoltaics with improved carrier extraction efficiency can be an answer to cheap solar energy.

In recent years, metal-organic frameworks (MOF) composed of metal clusters and organic linkers have been considered to be emerging materials for membrane gas separations. One critical challenge to achieve high-performance MOF membranes for gas separation is the great flexibility of the MOF struc-

ture, which can lead to breathing effects and linker rotation. Both phenomena can be induced by gas molecules permeating through the MOF channels, and result in changes of the pore-limiting diameter (PLD) of the MOF. This PLD is the window size for molecular transport; it determines the cut-off of

molecular sieving. This work led by Dun-Yen Kang (National Taiwan University) was aimed to create MOF membranes with great gas permeative selectivity via engineering the aperture size of a highly flexible MOF. Kang's team also combined experimental characterization and computational approaches to investigate how the adsorption of gas molecules in highly inhomogeneous pores affects the macroscopic permeation in MOF membranes.¹ They focused on an emerging pillared-bilayer MOF with great framework flexibility in this work. This MOF is composed of zinc as the metal cluster, 5-aminoisophthalic acid (aip) as the ligand to form the plated layer and 4,4'-azobipyridine (azpy) as the pillar ligand. The chemical formula of this compound is $\{[\text{Zn}_2(\text{azpy})(\text{aip})_2]\}_n$; this MOF is hereafter referred to as Zn-AIP-AZPY.

They conducted powder XRD measurements *in situ* on Zn-AIP-AZPY under various gases using the facilities at **TPS 09A**. These XRD patterns were obtained with an X-ray source of synchrotron radiation, which allows for a direct comparison of the peak intensities between the patterns. The results from the measurements under CO_2 and CH_4 are summarized in **Fig. 1**. They observed a remarkably decreased peak intensity as well as minor peak shifts in the XRD patterns of MA-48h with increasing partial pressure of CO_2 (**Fig. 1(a)**). The pronounced decrease of the peak intensity indicates the adsorption of CO_2 in Zn-AIP-AZPY. The occupation of gas molecules in the cage of MOF or any crystalline porous material decreases the electron density contrast within the materials, which leads ultimately to a decreased intensity of the powder XRD patterns. The peaks in the XRD patterns shifted towards smaller angles with increasing pressure of CO_2 , which might indicate a structural change of MA-48h subjected to the adsorption of CO_2 . In contrast with XRD measurements under CO_2 , the XRD patterns under CH_4 (**Fig. 1(b)**) presented no considerable change in either intensity or peak shift. This effect indicates a smaller adsorption of CH_4 in Zn-AIP-AZPY than of CO_2 , and implies also that CH_4 barely causes a structural deformation, unlike CO_2 .

The permeation properties of single gases H_2 , CO_2 , N_2 and CH_4 for both TA-24h and MA-48h are summarized in **Fig. 2**. As noted above, two methods of measurement were used: constant-pressure under feed pressure 2 bar (**Figs. 2(a) and 2(b)**) and constant-volume under feed pressure 0.5, 1 or 3 bar (**Figs. 2(c) and 2(d)**). The gas permeability was computed assuming a uniform membrane thickness, 70 μm . TA-24h (thermally activated for 24 h) possessed gas permeability

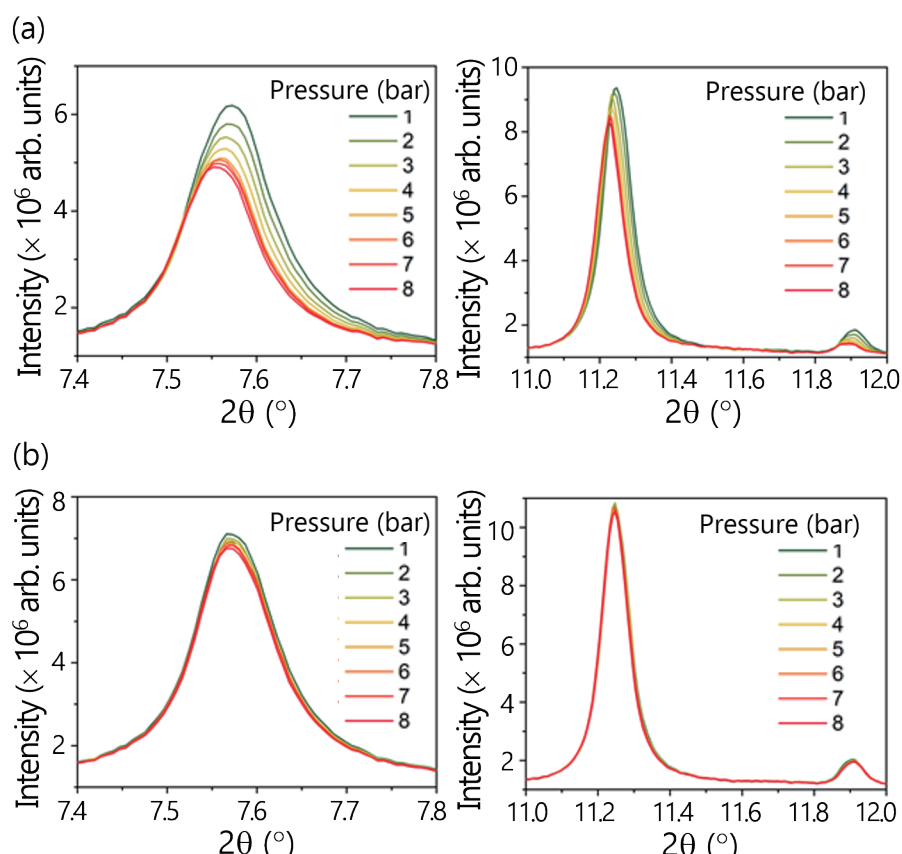
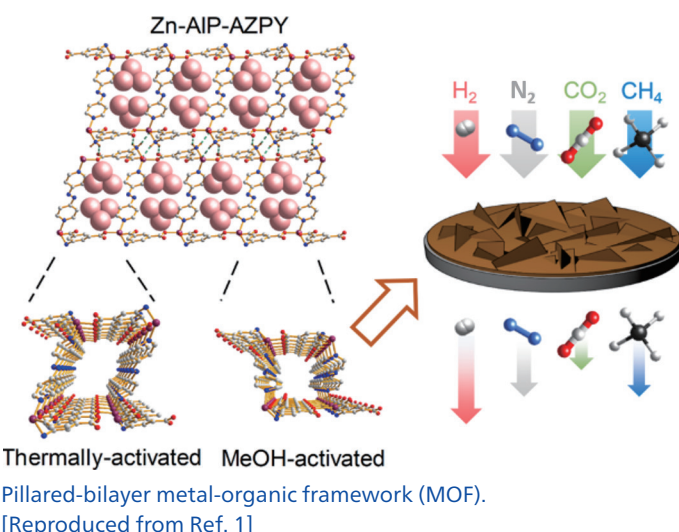


Fig. 1: Powder XRD patterns of Zn-AIP-AZPY obtained *in situ* under (a) CO_2 and (b) CH_4 at pressures ranging from 1 to 8 bar. The left panels show the patterns with 2θ between 7.4 and 7.8 $^\circ$; the right panels display the patterns with 2θ between 11.0 and 12.0 $^\circ$. [Reproduced from Ref. 1]

greater than MA-48h (methanol activated for 48 h) for all tested gases. The ideal selectivity, defined as the permeance ratio between two gases, of TA-24h for various gas pairs (H_2/CO_2 , N_2/CO_2 and CH_4/CO_2) was near the Knudsen selectivity. This result indicates that pinholes of size several nanometres might be present in the TA-24h membrane. In contrast, the ideal selectivity of MA-48h deviated from the Knudsen selectivity, indicating that its gas permeation is un-

likely to be dominated by pinholes; the grain boundary microstructure is properly controlled. The formation of pinholes in the TA-24h membrane might be due to the thermal treatment during the activation. We observed that the Zn-AlP-AZPY membrane sample collapses, an indication that the thermal activation is likely to create pinholes in the membranes. The permeability of the MA-48h membrane was, notably, considerably affected by the feed pressure (**Figs. 2(c) and 2(d)**): increasing

the feed pressure from 0.5 to 3 bar raised the permeability of CO_2 and CH_4 for the MA-48 membrane nearly two-fold, whereas the permeability of the TA-24h membrane remained approximately constant. These findings agree satisfactorily with the adsorption isotherms of these two samples, wherein the gate-opening effect was present in only MA-48h. The presence of the pinholes, of which the permeability is supposed not to be a function of pressure, in TA-24h can be also a reason that the overall permeability of TA-24h is unaffected by the feed pressure.

Overall, this work demonstrates the critical role of activation methods in controlling the structural topology and unravels the unique adsorption and permeation properties of Zn-AlP-AZPY owing to its structural flexibility. The insight obtained herein is expected to facilitate the development of flexible MOF in separation applications. (Reported by Dun-Yen Kang, National Taiwan University)

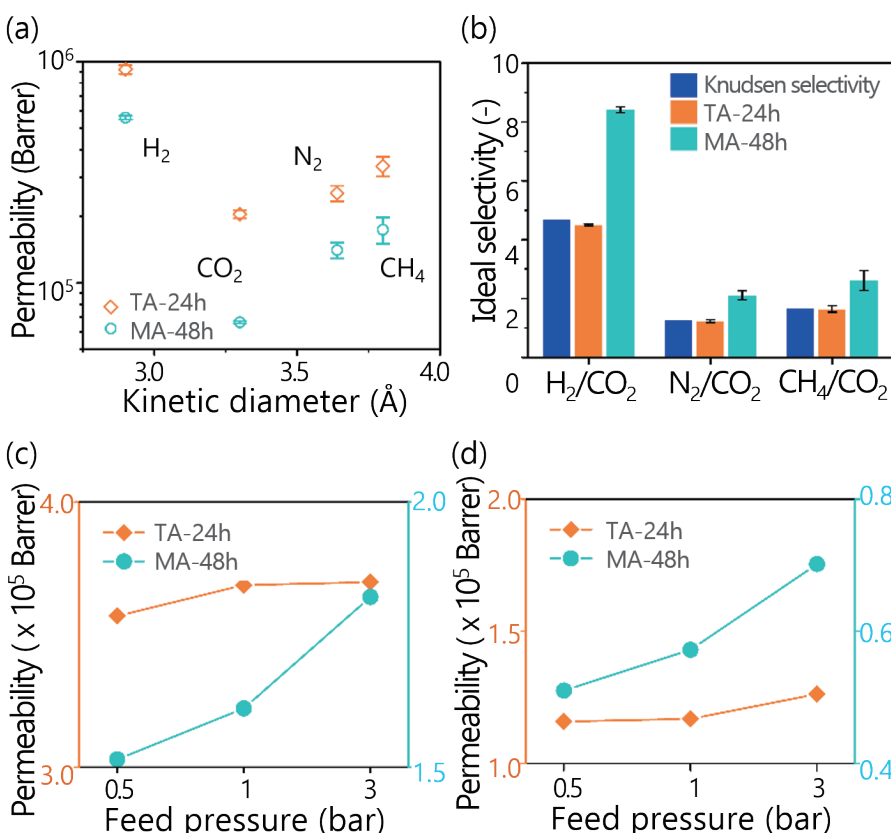


Fig. 2: (a) Single gas permeability and (b) ideal selectivity of Zn-AlP-AZPY membranes (TA-24h and MA-48h) with feed pressure 1 bar; (c) CH_4 and (d) CO_2 permeability of Zn-AlP-AZPY membranes under various feed pressures. [Reproduced from Ref. 1]



TPS 09A Temporally Coherent X-ray Diffraction.

This report features the work of Dun-Yen Kang and his collaborators published in *Chem. Mater.* **31**, 7666 (2019).

TPS 09A Temporally Coherent X-ray Diffraction

- XRD
- Materials Science, Chemical Engineering, Membrane, Membrane Gas Separation

Reference

1. M.-Y. Kan, J. H. Shin, C.-T. Yang, C.-K. Chang, L.-W. Lee, B.-H. Chen, K.-L. Lu, J. S. Lee, L.-C. Lin, D.-Y. Kang, *Chem. Mater.* **31**, 7666 (2019).